DESIGN AND NUMERICAL CHARACTERIZATION OF A NEW LEG EXOSKELETON FOR HUMAN NEUROMOTOR REHABILITATION

Cristian COPILUSI, Sorin DUMITRU, Ionut GEONEA, Florin COLICI, Nicolae DUMITRU

Abstract: This paper addresses attention to a design for an exoskeleton used on human locomotion purposes in case of people with neuromotor disorders. The design core is focused on two planar-parallel mechanisms implementation at the knee and ankle joints level of each leg exoskeleton. Thus, numerical simulations for the design process were carried out in order to validate the engineering feasibility of the proposed leg exoskeleton.
Key words: Leg Exoskeletons, Neuromotor Disorders, Kinematics, Planar- Parallel Mechanisms, Simulation.

1. INTRODUCTION

Nowadays exoskeletons are extensively used in medical rehabilitation programs and power augmentation systems. Some exoskeletons [3, 6] are fully actuated and involves all patient joints during rehabilitation programs. In case of the exoskeletons used on temporal recovery programs [9, 11] these can actuate individual joints from patient locomotion system (a single actuated joint, a pair of joints or a group of human lower limb joints).

Thus, for all exoskeletons it can be identified many design conditions for example: complex actuations, low or high cost principles, comfort during rehabilitation programs, user-friendly interface and easy operation features.

For the mentioned design conditions, some exoskeletons [3, 6] fulfill a part of them, other solutions [9, 12] cover the entire design conditions. The latest ones [9, 15] have a complex structure which leads to expensive rehabilitation programs for patients.

In major cases, due to the physician specific requirements, human exoskeletons have complex actuation mechanisms with a minimum number of actuators [2, 8, 9, 13]. Complex exoskeletons [8, 14, 15] have a simplified mechanical structure with all equivalent human locomotion system joints fully actuated by motors and a complex command&control program.

Thus, it can be identified two major objectives which the proposed leg exoskeleton have to accomplish in case of neuromotor rehabilitation programs namely: to have a fully actuated robotic system for walking activities and in particular cases to allow also motions on separate joints; to allow the physician to identify manually the locomotion system joints limit without any pain or injury occurred during neuromotor specific therapies. Second objective can be applied also on patients who anthropometric data cannot be identified from a motion pattern database.

By considering the imposed objectives, a feasibility study for designing a new leg exoskeleton, entitled NeuRob (Neuromotor Rehabilitation Robot), will be performed through this research and it is organized as follows. In the first section a state-of-the art analysis was accomplished with several leg exoskeleton solutions which can fulfill one of the desired objectives.

Second section is dedicated to an experimental analysis of human locomotion system in order to create a database with gait patterns used on leg exoskeleton design but also on exoskeleton command&control programs.

Based on the existent leg exoskeleton solutions, a conceptual exoskeleton design is proposed in third section especially dedicated to persons with neuromotor disorders for walking rehabilitation therapies. This has also to fulfill the proposed objectives.

A mathematical model for leg exoskeleton analysis in kinematic and dynamic conditions was elaborated in fourth section and the aim of this model was to obtain reaction and connection forces which will be further used as input data on virtual simulations.

Thus for validating the proposed leg exoskeleton, a numerical processing was carried out and the obtained results validate the feasibility analysis and also the proposed leg exoskeleton model.

2. HUMAN WALKING EXPERIMENTAL ANALYSES

By having in sight the objectives imposed on the leg exoskeleton design, it is necessary to have a database with human gait patterns and anthropometric data from a group of healthy persons. Thus, a group of 30 healthy persons (15 male and 15 female) with ages between 30 to 58 years old, weight between 55 kilograms and 95 kilograms, height from 1.55 meters to 1.90 meters, were chosen for the experimental analysis and database development. The experimental analyses were performed and numerically processed with the aid of ViCON equipment from University of Craiova Research Centre – Biomechanical laboratories [16, 19]. For this, a protocol was created and the workflow is schematized in Fig. 1.

This protocol consists of: preparing the person for experimental tests; VICON equipment setup; calibrating cameras and positioning the global reference system; numerical data processing; acquiring the filtered angular data and exporting these as a report of each experimental test.

According with the experimental analysis workflow, each analyzed human subject wear a special suit with 52 characteristic markers which allow VICON cameras to identify in real-time mode the position, speed and accelerations of each attached marker during experimental analysis development. VICON Equipment has 14 high-speed cameras which can track and

record the attached markers on each human subject. These cameras works in IR-mode with a frame rate of 1000 frames/second.
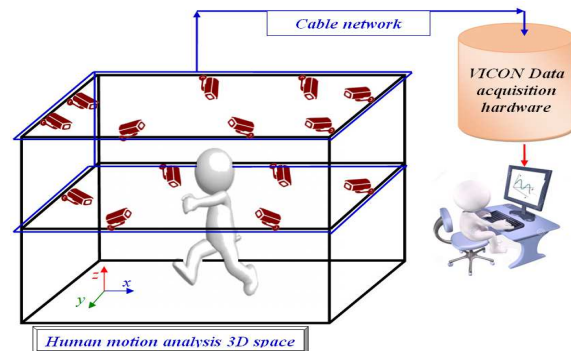
Fig. 1. VICON equipment workflow

For a case study we consider a female human subject with known anthropometric data (age 31 years, dimensional leg parameters known, 61 kilograms weight, 1.75meters height). In case of this person, a complete gait was performed in a time period of 1.45seconds. This time period it is important to know for virtual simulations of the designed exoskeleton.

In case of the processed data, these were represented by angular variations of each joint from human locomotion system, in a simultaneous mode for hips, knees and ankle joints. For the proposed female subject these are presented in Fig. 2, to Fig. 4.

In particular, from Fig. 2 one can observe that the angular variation for human hip joints is between -23.6575 degrees to19.537 degrees. In case of Fig. 3, the angular variation of a human knee motion during a single gait is between 0 to 51.261 degrees. By analyzing Fig. 4, the angular variation in case of human ankle joint motion during one gait is between -33.237degrees to 32.428 degrees.
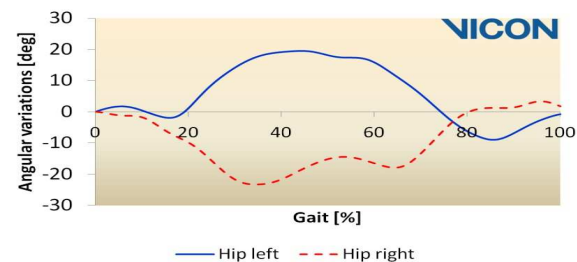
Fig. 2. Hip joints angular variations during one gait vs. time
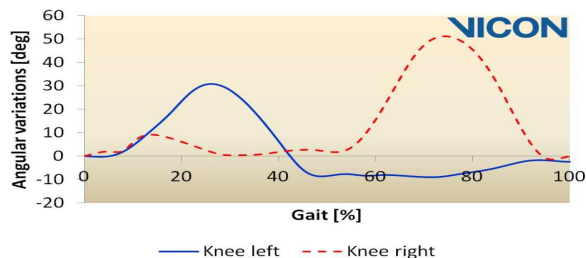
Fig. 3. Knee joints angular variations during one gait vs. time
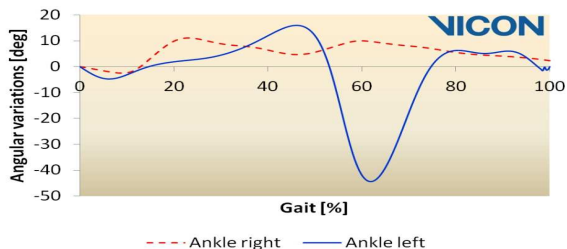
Fig. 4. Ankle joints angular variations during one gait vs. time

Also these are useful for carrying out corresponding validation between numerical computation and experimental analysis. In order to validate the obtained results, by comparing them with specialty literature data [17, 19, 20, 21, 22] these are presented in degrees as measuring units. Thus, for further use as input data, these will be converted in Radians as measuring units. The starting position for the recorded data in case of the proposed experimental tests has been considered when the heel has the first contact with the ground.

3. A NEW LEG EXOSKELETON MECHANISM

By considering existing solutions for leg mechanisms [7, 8, 13] a new leg exoskeleton mechanism can be conceived as to be fairly simple, easy to wear and to adapt to a human leg. The proposed leg exoskeleton mechanism is presented in a structural scheme from Fig. 5. For this solution there are used three actuators for each equivalent human joint namely hip, knee and ankle joints. These are placed as it follows: two actuators for moving the hip joint O and knee joint mechanism which is created by first planar-parallel mechanism, namely OABCDEF.
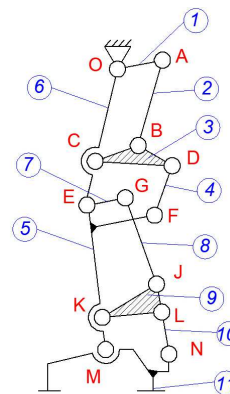
Fig. 5. A structural scheme for a new leg exoskeleton mechanism with two planar-parallel actuating mechanisms

Other actuator is placed at the knee joint level, but it actuates the second planar-parallel mechanism, respectively the one of EGJKLMN. Also it can be remarked that there are a number of 11 links and all joints are revolute ones. The equivalent link for the femur is the link no 6, tibia is equivalent to the link no 5 and foot segment is equivalent to the link no 11. In this manner it can be considered common joints the ones from O (it corresponds to the hip joint actuation, but it serve also as a support for first planar-parallel mechanism actuation) and the ones from E (it corresponds to the knee joint actuation, but it serve also as a support for second planar-parallel mechanism actuation). It is well known that the human leg perform angular motions around the main joints, but there is no joint that can perform a 360 degrees rotation. If we choose proper revolute actuators, these can perform 360 degrees and more. From this viewpoint arises the motivation of choosing these mechanisms which represent a mechanical limit imposed by the link no 1 and link no 7, if the actuators will rotate continuously. In case of knee actuation, the motion is transmitted from link no 1 to tibia equivalent link no 5 through the first planar-parallel linkage made by links no 2, 3, and 4. For ankle actuation, the motion will be transmitted from link no 7 to foot equivalent link no 11 through the second planar-parallel linkage made by links no 8, 9, 10 and 11.

An advantage of the proposed leg exoskeleton is the one that the actuator units can be placed on a separated frame at a proper distance from the human legs and the motions can be transmitted through chain transmissions.

In addition, link sizes can be parameterized in order to adjust them for adapting to a large category of persons.

Thus, it is necessary to understand that during gait process each human foot is in contact with the ground and due to this argument, the entire leg exoskeleton needs three actuators, according with Fig. 5. If the foot and ground forms a rolling without friction contact, then the mechanism needs a single actuator. In case of the foot and ground forms a rolling with friction contact, then the mechanism needs two actuators. Thus, the advantage of using these actuation mechanism types will allow reproducing a precise foot motion with differentiated energy consumption for some gait sequences during human walking.

4. LEG EXOSKELETON KINEMATIC ANALYSIS

For the proposed leg exoskeleton mechanism, there were elaborated two kinematic schemes presented in Fig. 6. By taking into account a kinematic method [7, 8] based on Newton-Raphson algorithm for spatial and planar mechanism kinematic analysis, there were considered as input data, the obtained angular variations for hip, knee and ankle joints.
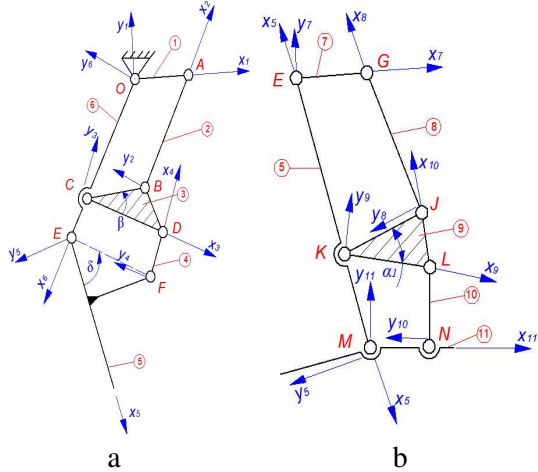
Fig. 6. Kinematic schemes for knee joint mechanism (a), and ankle joint mechanism (b)

These were obtained through experimental analysis from the proposed human subject. In this kinematic analysis frame, these angular variations are renamed with the φ_{06}, φ_{65}, φ_{57} symbols and represents equations in a polynomial form. Based on these known angular variations, the kinematic analysis will be an inverse one and the purpose of this is to obtain the actuators motion variation laws and angular speeds. First step on this analysis is to obtain the position of each link and for this each kinematic link will be attach a reference system with a proper versor base. Thus, the transformation equations for crossing from a reference system to another will be written as it follows:

$$A_{ij} = \begin{bmatrix} \cos\phi_{ij} & -\sin\phi_{ij} \\ \sin\phi_{ij} & \cos\phi_{ij} \end{bmatrix}$$ (2)

φ_{ij}- rotation angle between reference system unghiul T_i and T_j, with the z_i sand z_j, common axis.

Based on the matrices from (2), it can be identified the versors base from crossing from a reference system to another in case of knee planar-parallel actuation mechanism:

$$\vec{W}_6 = A_{06} \cdot \vec{W}_0; \quad \vec{W}_5 = A_{65} \cdot \vec{W}_6 = A_{65} \cdot A_{06} \cdot \vec{W}_0;$$

$$\vec{W}_5 = A_{05} \cdot \vec{W}_0; \quad A_{05} = A_{06} \cdot A_{65}; \quad \vec{W}_4 = A_{54} \cdot \vec{W}_5;$$

$$\vec{W}_3 = A_{63} \cdot \vec{W}_6 = A_{63} \cdot A_{06} \cdot \vec{W}_0;$$

$$\vec{W}_3 = A_{03} \cdot \vec{W}_0; \quad A_{03} = A_{63} \cdot A_{06};$$

$$\vec{W}_2 = A_{32} \cdot \vec{W}_3 = A_{32} \cdot A_{03} \cdot \vec{W}_0;$$

$$\vec{W}_2 = A_{02} \cdot \vec{W}_0; \quad A_{02} = A_{32} \cdot A_{03}; \quad \vec{W}_1 = A_{01} \cdot \vec{W}_0;$$ (3)

For ankle and foot actuating mechanism, the versors base attached to kinematic links are expressed by:

$$\vec{W}_6 = A_{06} \cdot \vec{W}_0; \vec{W}_5 = A_{65} \cdot \vec{W}_6 = A_{65} \cdot A_{06} \cdot \vec{W}_0 = A_{05} \cdot \vec{W}_0;$$

$$\vec{W}_{11} = A_{511} \cdot \vec{W}_5 = A_{511} \cdot A_{05} \cdot \vec{W}_0 = A_{011} \cdot \vec{W}_0;$$

$$\vec{W}_{10} = A_{1110} \cdot \vec{W}_{11} = A_{1110} \cdot A_{011} \cdot \vec{W}_0 = A_{010} \cdot \vec{W}_0;$$

$$\vec{W}_9 = A_{59} \cdot \vec{W}_5 = A_{59} \cdot A_{05} \cdot \vec{W}_0 = A_{09} \cdot \vec{W}_0;$$

$$\vec{W}_8 = A_{98} \cdot \vec{W}_9 = A_{98} \cdot A_{09} \cdot \vec{W}_0 = A_{08} \cdot \vec{W}_0;$$

$$\vec{W}_7 = A_{57} \cdot \vec{W}_5 = A_{57} \cdot A_{05} \cdot \vec{W}_0 = A_{07} \cdot \vec{W}_0;$$ (4)

There will be identified the kinematic constraints Equations starting from general form as:

$$\varphi_i(q,t) = 0 \ , \ i = \overline{1,8} \qquad (5)$$

Where: t is time and q are generalized coordinates.

By particularizing the general form of Eq. (5) it can be written the following Eq. system:

$$\varphi(q,t) = \begin{cases} cos\,\varphi_{54}\,X_{D4} - sin\,\varphi_{54}\,Y_{D4} + cos\,\varphi_{65}\,X_{F5} - sin\,\varphi_{65}\,Y_{F5} + cos\,\varphi_6\,X_{E6} - sin\,\varphi_6\,Y_{E6} - \\ - cos\,\varphi_{63}\,X_{D3} + sin\,\varphi_{63}\,Y_{D3} - cos\,\varphi_6\,X_{C6} + sin\,\varphi_6\,Y_{C6} \\ sin\,\varphi_{54}\,X_{D4} + cos\,\varphi_{54}\,Y_{D4} + sin\,\varphi_{65}\,X_{F5} + cos\,\varphi_{65}\,Y_{F5} + sin\,\varphi_6\,X_{E6} + cos\,\varphi_6\,Y_{E6} - \\ - sin\,\varphi_{63}\,X_{D3} - cos\,\varphi_{63}\,Y_{D3} - sin\,\varphi_6\,X_{C6} - cos\,\varphi_6\,Y_{C6} \\ cos\,\varphi_{32}\,X_{A2} - sin\,\varphi_{32}\,Y_{A2} + cos\,\varphi_{63}\,X_{B3} - sin\,\varphi_{63}\,Y_{B3} + cos\,\varphi_6\,X_{C6} - sin\,\varphi_6\,Y_{C6} - \\ - cos\,\varphi_1\,X_{A1} + sin\,\varphi_1\,Y_{A1} \\ sin\,\varphi_{32}\,X_{A2} + cos\,\varphi_{32}\,Y_{A2} + sin\,\varphi_{63}\,X_{B3} + cos\,\varphi_{63}\,Y_{B3} + sin\,\varphi_6\,X_{C6} + cos\,\varphi_6\,Y_{C6} - \\ - sin\,\varphi_1\,X_{A1} - cos\,\varphi_1\,Y_{A1} \\ sin\,\varphi_{98}\,X_{G8} + cos\,\varphi_{98}\,Y_{G8} + sin\,\varphi_{59}\,X_{J9} + cos\,\varphi_{59}\,Y_{J9} + sin\,\varphi_{65}\,X_{K5} + cos\,\varphi_{65}\,Y_{K5} - \\ - sin\,\varphi_{57}\,X_{G7} - cos\,\varphi_{57}\,Y_{G7} \\ X_{L10}\,cos\,\varphi_{l110} - Y_{L10}\,sin\,\varphi_{l110} + cos\,\varphi_{511}\,X_{N11} - sin\,\varphi_{511}\,Y_{N11} + cos\,\varphi_{65}\,X_{M5} - \\ - sin\,\varphi_{65}\,Y_{M5} - cos\,\varphi_{59}\,X_{L9} + sin\,\varphi_{59}\,Y_{L9} - cos\,\varphi_{65}\,X_{K5} + sin\,\varphi_{65}\,Y_{K5} \\ sin\,\varphi_{l110}\,X_{L10} + sin\,\varphi_{l110}\,Y_{L10} + sin\,\varphi_{511}\,X_{N11} + cos\,\varphi_{511}\,Y_{N11} + sin\,\varphi_{65}\,X_{M5} + \\ + cos\,\varphi_{65}\,Y_{M5} - sin\,\varphi_{59}\,X_{L9} - cos\,\varphi_{59}\,Y_{L9} - sin\,\varphi_{65}\,X_{K5} - cos\,\varphi_{65}\,Y_{K5} \\ cos\,\varphi_{98}\,X_{G8} - sin\,\varphi_{98}\,Y_{G8} + cos\,\varphi_{59}\,X_{J9} - sin\,\varphi_{59}\,Y_{J9} + cos\,\varphi_{65}\,X_{K5} - sin\,\varphi_{65}\,Y_{K5} - \\ - cos\,\varphi_{57}\,X_{G7} + sin\,\varphi_{57}\,Y_{G7} \end{cases}$$

$$(6)$$

Thus, it will be obtained:

$$q = \left\{ \varphi_{01}, \varphi_{32}, \varphi_{54}, \varphi_{63}, \varphi_{98}, \varphi_{59}, \varphi_{1110}, \varphi_{57} \right\}^T \qquad (7)$$

The mathematical model presented through this kinematic analysis has a flexible character and it can be easily implemented through an algorithm with the use of MAPLE. In this way, the entire mathematical model can be parameterized with the anthropometric data of the proposed human subject and with the angular variations of the analyzed joints (hip, knee and ankle joint for the left lower limb). The input data can be expressed as geometrical characteristics of each kinematic link as it follows: β=18.51[radians]; δ=35.47 [radians]; α=35.47 [radians]; l_{OC}= 391mm; l_{OE}= 411.11mm; l_{OA}= 22.13mm; l_{AB}= 371.1mm; l_{BD}= 29.41mm; l_{BC}= 39.18mm; l_{DC}= 63.8mm; l_{CE}= 50.99mm; l_{EF}= 63.85mm; l_{DF}= 90mm; l_{JG}= 384.35mm; l_{EK}= 389.53mm; l_{EM}= 441.35mm; l_{MN}= 71.35mm; l_{LN}= 66.45mm; l_{KJ}= 74.29mm; l_{GJ}= 384.35mm; l_{EG}= 55mm.

Hip angular variation was labeled with the term of φ_{06}, knee angular was also represented by the term of φ_{65} and in case of ankle joint angular variation, this was labeled with φ_{511} term. These joints angular variations can be expressed by the following polynomial

Equations according with the parameterized model:

$$\varphi_{06} = 0.05436169159 - 1.049144646 \cdot t + \\ + 3.528717373 \cdot t^2 + 4.459178549 \cdot t^3 - \\ - 16.81669021 \cdot t^4 + 12.95743095 \cdot t^5 - \\ - 3.037974275 \cdot t^6 \qquad (8)$$

$$\varphi_{65} = 0.05572857950 - 3.917643736 \cdot t + \\ + 46.09421696 \cdot t^2 - 142.2026539 \cdot t^3 + \\ + 183.2410652 \cdot t^4 - 106.6799384 \cdot t^5 + \\ + 23.24793765 \cdot t^6 \qquad (9)$$

$$\varphi_{511} = 0.007468922928 + 4.125887507 \cdot t - \\ - 46.18350162 \cdot t^2 + 139.7502390 \cdot t^3 - \\ - 185.4096885 \cdot t^4 + 113.2636093 \cdot t^5 - \\ - 25.99845833 \cdot t^6 \qquad (10)$$

On Eqs. (8), (9) and (10) it can be remarked that these angular variations are converted in radians. This conversion was done for using these in MSC Adams environment, due to the created model which supports only [radians] as input data for units. These have the paths presented on diagrams from Figs. 7, 8 and 9.

A first remark of the plotted results from Figs. 7, 8 and 9 is the one that these have similar paths like those obtained from experimental tests of the proposed human subject for left lower limb.

The output of the mathematical model computation is to obtain the actuators motion laws for the parameterized model in case of

actuating the knee planar-parallel mechanism and ankle planar-mechanism.
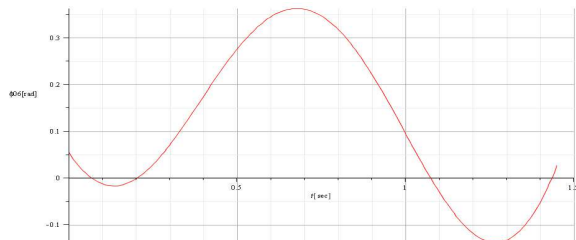
Fig. 7. Hip joint angular variation diagram equivalent to φ_{06} angle vs. time
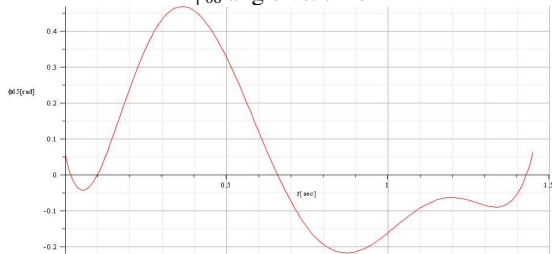
Fig. 8. Knee joint angular variation diagram equivalent to φ_{65} angle vs. time
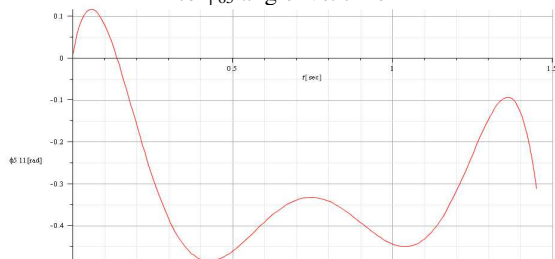
Fig. 9. Ankle joint angular variation diagram equivalent to φ_{511} angle vs. time

These important data will be used for virtual simulations of the proposed leg exoskeleton 3D model with the aid of MSC Adams. The targeted actuator motion angular variations will be φ_{01} and φ_{57}. These results are plotted in diagrams from Fig. 10 and 11. Furthermore these also will be used for motion control on the acquired servomotor units.
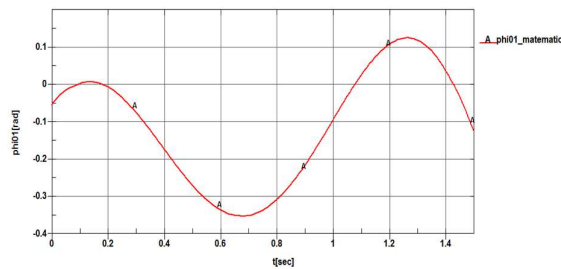
Fig. 10. Motion law of the drive link for knee actuation mechanism equivalent to φ_{01} angle vs. time
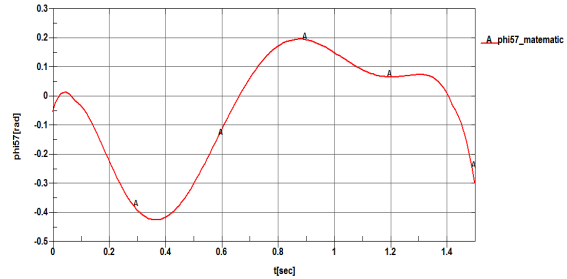
Fig. 11. Motion law of the drive link for ankle actuation mechanism equivalent to φ_{57} angle vs. time

5. LEG EXOSKELETON MODELLING AND SIMULATIONS

A virtual model of the new leg exoskeleton mechanism has been created in SolidWorks according to the kinematic schemes from Fig. 8 and structural scheme from Fig. 6. This is shown in Figs. 12 and 13 as related to the exoskeleton design in all its components. Also in Fig. 12 can be remarked the correspondence between the structural scheme and the 3D model of left exoskeleton leg.

By taking into account the structural scheme from Fig. 6, it can be easily identified the correspondence between components from Fig. 12. A leg exoskeleton from Fig. 12 has been built with 15 revolute joints and 11 links. Three revolute actuators are considered for the operation of each leg exoskeleton system and the entire exoskeleton will be actuated by six servomotor units placed in an additional frame on the back of the patient as it can be remarked in Figure 13.
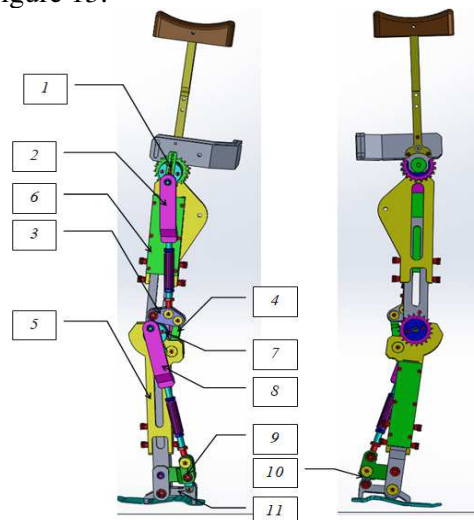
Fig. 12. A 3D model of the proposed leg exoskeleton

Thus, in Figure 13 the following subassemblies are identified: 1 – servomotors unit for actuating the left leg exoskeleton; 2 – additional frame support; 3 – left leg of the 3D exoskeleton; 4 - servomotors unit for actuating the right leg exoskeleton; 5 – right leg of the 3D exoskeleton. The entire exoskeleton was imported in MSC Adams – Adams View [18] module for virtual simulations as it is shown in Figure 14.
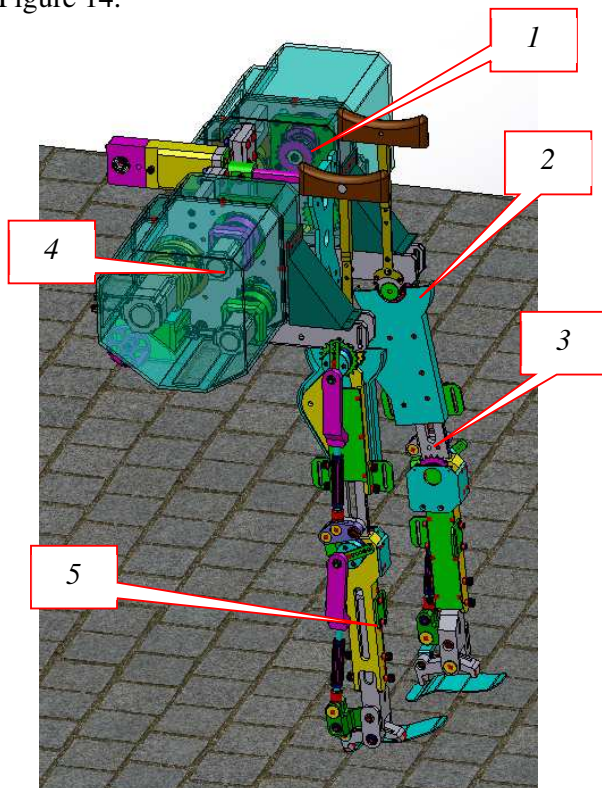
Fig. 13. NeuRob entire virtual model

All links were considered as made from aluminum alloys with proper mechanical characteristics, namely elasticity module ($E=6.9 \times 10^5$ MPa), density ($2705 kg/m^3$) and Poisson ratio (0.33). There were defined 15 revolute joints between the exoskeleton links and 6 motor joints (two for hips, two for drive links of the planar-parallel mechanisms for knee actuation and two for drive links of the planar-parallel mechanisms for ankle actuation). The joint friction force was considered with the following parameters: static coefficient equal with 0.01; dynamic coefficient with 0.005; stiction transition velocity equal to 0.1; maximum stiction deformation as 0.01.

There were considered two major virtual simulations stages: first stage when there were inserted the actuation motion laws namely φ_{01}, φ_{57} obtained from the processed mathematical model, namely Fig. 10 and Fig. 11; second stage when there were inserted the angular motion laws on hip, knee, ankle joints and the desired results was to obtain angular variations of φ_{01}, φ_{57}, only for certify that the prepared 3D exoskeleton model is valid for virtual simulations.

For the first stage, a major remark is the one that these drive motion laws for the left exoskeleton leg were defined in the presented form from the mentioned figures, but in case of right exoskeleton leg, these were mirrored as diagrams and with the aid of MAPLE there were obtained tabular data and after this the polynomial form. In case of hip joints there were inserted the polynomial form of the presented motion laws from Fig. 2 from experimental analysis.

For second stage there were inserted the motion laws obtained from experimental analysis namely the ones from Fig. 2, Fig. 3 and Fig. 4 in order to obtain, as a verifying point, for the actuation motion laws namely φ_{01}, φ_{57}. Second stage represents a direct kinematic analysis with the Adams software and there were obtained motion variation laws depending on time without any additional loads.
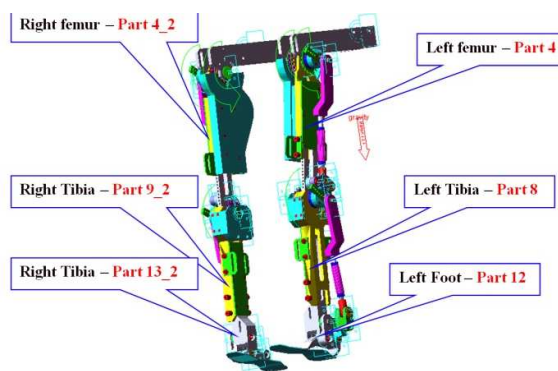
Fig. 14. 3D model of the proposed exoskeleton prepared for virtual simulations for the first stage

Also this stage is useful to obtain motion laws for command&control unit program and for certify that the experimental analyses were performed in optimum conditions for walking analysis. In addition from second stage there

were obtained more parameters used on further researches for inverse dynamic analysis or kinematic optimization processes of the NeuRob.

The kinematic setup sequence was defined for a time interval of 1.45seconds. Some snapshots during virtual simulations for the first stage are shown in Fig. 15.

Data post processing represents the final step for accomplishing the research objectives. Thus, there were determined kinematic motion variation laws in case of femur, tibia and foot segments for both exoskeleton legs in case of second stage developed under MSC – Adams/Adams View module. These parameters were obtained during a single gait and it represents the displacement components of the identified mass centers from Fig. 16 of the interest segments for y-horizontal axis, z-vertical axis and Euler angles (where θ is a variable angle) but also the ω - angular speed of the x-axis perpendicular on the created yz plane.

Numerical results of the simulation for the first stage are reported in the plots from Fig. 16 and Fig. 17 as related to the third step of the simulated walking. This step corresponds with the one from experimental tests and also the time period was setup to 1.45 seconds.

Dyna processor which allow importing tabular data from MAPLE and Adams graphs as it can be observed from Fig. 16 and Fig. 17. At a first look in case of the comparison between mathematical model and virtual simulations from Adams environment, in Fig. 16 both curves have the same paths and the accuracy was under 1%. These reported data corresponds for actuation mechanism of the knee joint.
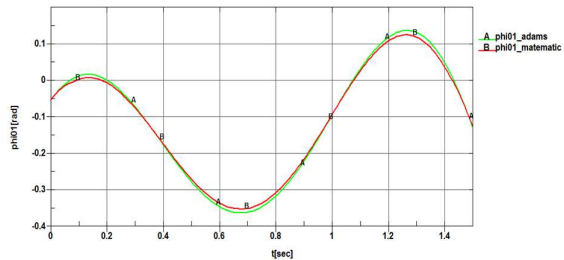
Fig. 16. A comparison between Adams model and mathematical model of the angular motion variation law for O joint, namely φ_{01}, vs time

In case of ankle and foot actuation from Fig. 17 it can be remarked that the comparison between mathematical model and virtual simulations from Adams environment has accuracy under 3%. The obtained curves have also similar paths.
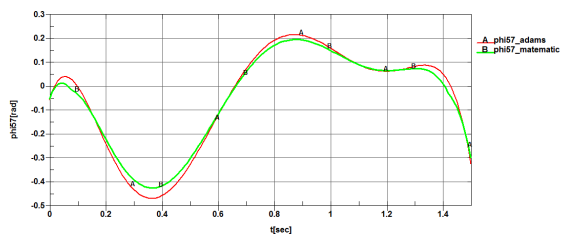
Fig. 17. A comparison between Adams model and mathematical model of the angular motion variation law for E joint, namely φ_{57}, vs time

Fig. 15. Snapshots during virtual simulations for a single gait of the proposed exoskeleton

For a comparison analysis it was used a module from ANSYS software, namely LS-

These actuation motion laws where further used to command and control the NeuRob exoskeleton. Summarizing, the obtained results through the reported numerical simulation show a characteristic functioning of the entire exoskeleton with proper values and behavior as function of the operation of all its components when acting in an assisting operation with a human user.

Thus, in Fig. 18 it is presented the real prototype of the NeuRob exoskeleton.
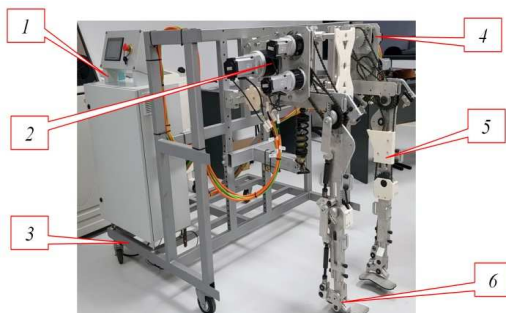
Fig. 18. NeuRob exoskeleton real prototype

This has the following major components: 1 – command&control unit; 2 – servomotors unit for right leg of NeuRob exoskeleton; 3 – base frame; 4 - servomotors unit for left leg of NeuRob exoskeleton; 5 – left leg of NeuRob exoskeleton; 6 – right leg of NeuRob exoskeleton.

6. CONCLUSIONS

A new design solution is proposed for a leg exoskeleton mechanism which is based on planar-parallel mechanism.

A novelty of the exoskeleton design is related to the actuating mechanism which protect the entire structure from any human risk of accidents.

A database for human gait analysis was obtained on experimental way with the aid of a VICON equipment for a set of 30 human healthy subjects and this is useful on creating gait patterns for several persons with different anthropometric data.

It was created a mathematical algorithm based on Newton-Raphson formalism for leg exoskeleton kinematic analysis. Thus, a program with a flexible character was written, under MAPLE environment. Through this program there were identified the angular variation laws of the drive joints of the proposed leg exoskeleton model, but also angular speeds and accelerations furthermore used in dynamic analyses.

A characterization of the exoskeleton operation has been outlined by reporting numerical results of the simulation performing an assisting operation of the exoskeleton during walking activity.

The obtained results validate the proposed leg exoskeleton and the feasibility study was done by obtaining the NeuRob exoskeleton real prototype.

8. REFERENCES

[1] A. Esquenazi, M. Talaty, A. Jayaraman, *Powered exoskeletons for walking assistance in persons with central nervous system injuries: a narrative review*, PM & R9. 2017. pp. 46–62.

[2] D.R. Louie, J.J. Eng, "Powered robotic exoskeletons in post-stroke rehabilitation of gait: a scoping review", *J. Neuroeng. Rehabil*. Vol. 13/53. 2016.

[3] M. Bortole, A. Venkatakrishnan, F. Zhu, et. al., *The H2 robotic exoskeleton for gait rehabilitation after stroke: early findings from a clinical study*. Journal of NeuroEngineering and Rehabilitation. Vol. 12:54. 2015. pp. 1-14.

[4] S. Federici, F. Meloni, M. Bracalenti, M.L. De Filippis, *The effectiveness of powered, active lower limb exoskeletons in neurorehabilitation: a systematic review*. Journal of Neuro-Rehabilitation. Vol. 37. 2015. pp. 321–340.

[5] Pons JL. *Wearable robots: biomechatronic exoskeletons*. Chichester, UK: John Wiley & Sons, Ltd, 2008.

[6] Banala SK, Agrawal SK and Scholz JP., "Active leg exoskeleton (ALEX) for gait rehabilitation of motor-impaired patients". *In IEEE 10th international conference on rehabilitation robotics* (eds B Driessen, JL Herder, GJ Gelderblom), 13–15 June 2007, Noordwijk, Netherlands, pp. 401–407. IEEE. DOI: 10.1109/ICORR.2007.4428456

[7] Dumitru N., A. Didu, C. Copilusi, *Mechatronic system for locomotion rehabilitation*. Advances in Engineering and Management. ISSN 2537- 4443. 2016. pp. 53-54.

[8] Dumitru N., Copilusi C., Geonea I., et. al., *Dynamic Analysis of an Exoskeleton New*

Ankle Joint Mechanism. In: Flores P., Viadero F. (eds) New Trends in Mechanism and Ma-chine Science. Mechanisms and Machine Science, vol 24. Springer. 2015

[9] Yu S, Han C and Cho I., *Design considerations of a lower limb exoskeleton system to assist walking and load-carrying of infantry soldiers*. Appl Bion Biomech 2014; 11(3): 119–134.

[10] Lopez R, Aguilar H, Salazar S, et al., *Modelado y Control de un Exoesqueleto para la Rehabilitacio´n de Extremidad Inferior con dos grados de libertad*. Rev Iberoam Automatica e Informatica Ind RIAI 2014; 11(3). pp. 304–314.

[11] Galle S, Malcolm P, Derave W, et al., *Adaptation to walking with an exoskeleton that assists ankle extension*. Gait Posture. 2013; 38(3). pp. 495–499.

[12] Strausser KA, Zoss AB, Swift TA, et al., *Mobile exoskeleton for spinal cord injury: development and testing*. In Proceedings of the ASME 2011 dynamic systems and control conference, Arlington, VA, USA, 31 October–2 November 2011, pp. 419–425. DOI: 10.1115/DSCC2011-6042

[13] Geonea, I. D., Margine, A., Dumitru, N., Copiluşi, C., *Design and simulation of a mechanism for human leg motion assistance*. In Advanced Materials Research Vol. 1036, pp. 811-816. 2014.

[14] Ghobrial GM and Wang MY., *The next generation of powered exoskeleton use in spinal cord injury*. Neurosurg Focus 2017; 42(5): E16.

[15] S.H.You, *Concurrent Validity and Test-Retest Reliability of the Novel Walkbot-K System*. J. Mech. Med. Biol. 16. 2016.

[16] VICON Motion Analysis Equipment *User Manual* Accessed in 2016.

[17] Pirker, W., Katzenschlager, R., *Gait disorders in adults and the elderly: A clinical guide*. Wiener klinische Wochenschrift. 2016. 129.10.1007/s00508-016-1096-4.

[18] MSC Adams software *User Manual*. Accessed in 2017.

[19] Steinicke F, Visell Y, Campos J, et al., *Human walking in virtual environments*. New York, NY, USA: Springer, 2013.

[20] Duffy J., *Statics and kinematics with applications to robotics*. New York, NY, USA: Cambridge University Press, 1996, pp. 173.

[21] Muscolo G., Caldwell D., Cannella F. Biomechanics of Human Locomotion with Constraints to Design Flexible-Wheeled Biped Robots. IEEE International Conference on Advanced Intelligent Mechatronics. pp1273 – 1278. 2017.

[22] Arturo Bertomeu-Motos. Biomechanics of human walking and stability descriptive parameters. Biomedical Neuroengineering Research Group. Revista Doctorado UMH. Vol. 1 no. 1. pp. 4-8. 2015.

PROIECTAREA ȘI CARACTERIZAREA NUMERICĂ A UNUI NOU EXOSCHELET PICIOR PENTRU REABILITAREA NEUROMOTORIE UMANĂ

Rezumat: Această lucrare acordă atenție unui design pentru un exoschelet folosit în scopuri de locomoție umană în cazul persoanelor cu tulburări neuromotorii. Nucleul de proiectare se concentrează pe punerea în aplicare a două mecanisme planare-paralele la nivelul articulațiilor genunchiului și gleznei din fiecare exoschelet picior. Astfel, au fost efectuate simulări numerice pentru procesul de proiectare în vederea validării fezabilității inginerești a exoscheletului de etapă propus

Copilusi Cristian, Assoc. Prof. PhD. Eng, Vice-dean, University of Craiova, Faculty of Mechanics, cristian.copilusi@edu.ucv.ro, +40747222771, Calea Bucuresti 107. Craiova. Romania.

Dumitru Sorin, Lecturer. PhD. Eng., University of Craiova, Faculty of Automation, Computers and Electronics, sorin.dumitru@edu.ucv.ro, +40744152497, Decebal 107. Craiova. Romania.

Geonea Ionut, Assoc. Prof. PhD. Eng., University of Craiova, Faculty of Mechanics, ionut.geonea@edu.ucv.ro, +40727779866, Calea Bucuresti 107. Craiova. Romania.

Colici Florin, PhD student. Eng., University of Craiova, Faculty of Mechanics, florin.colici@gmail.com, +40747363385, Calea Bucuresti 107. Craiova. Romania.

Dumitru Nicolae, Prof. PhD. Eng, Vice-rector, University of Craiova, nicolae.dumitru@edu.ucv.ro, +40740084392, A.I. Cuza 13. Craiova. Romania.